Chemical Engineering Journal 241 (2014) 52–59

Contents lists available at ScienceDirect

Chemical Engineering Journal

journal homepage: www.elsevier.com/locate/cej

Effect of support on the deep oxidation of propane and propylene on Pt-based catalysts

M.S. Avila, C.I. Vignatti, C.R. Apesteguía *, T.F. Garetto *

Catalysis Science and Engineering Research Group (GICIC), INCAPE, UNL-CONICET, Santiago del Estero 2654, 3000 Santa Fe, Argentina[1]

HIGHLIGHTS

- The Pt-supported catalyst activity for C_3H_8 and C_3H_6 oxidations depends on the nature of both the reactant and the support.
- The propane combustion turnover rate trend is $Pt/TiO_2 > Pt/CeO_2 > Pt/Al_2O_3$.
- The higher C_3H_8 oxidation rate on Pt/TiO_2 probably reflects the higher C_3H_8 uptake on TiO_2.
- The propylene combustion turnover rate trend is $Pt/CeO_2 > Pt/Al_2O_3 \cong Pt/TiO_2$.
- The higher C_3H_6 oxidation rate on Pt/CeO_2 is explained by an additional oxidation pathway on Pt^0–Ce^{3+} sites.

ARTICLE INFO

Article history:
Received 2 September 2013
Received in revised form 2 December 2013
Accepted 3 December 2013
Available online 10 December 2013

Keywords:
Propane oxidation
Propylene oxidation
Hydrocarbon combustion
Pt-based catalysts
Environmental catalysis

ABSTRACT

The complete oxidations of propane and propylene were studied on Pt supported on CeO_2, TiO_2 and Al_2O_3. The catalyst activities were evaluated through conversion versus temperature (light-off curves) and conversion versus time tests. Propane oxidation turnover rates (TOF) followed the order: $Pt/TiO_2 > Pt/CeO_2 > Pt/Al_2O_3$. The higher activity on Pt/CeO_2 than on Pt/Al_2O_3 was interpreted by considering that the combustion of C_3H_8 on Pt/CeO_2 occurs not only on Pt^0 sites but also on perimeter Pt^0–Ce^{3+} sites providing an additional oxidation pathway. Propane uptake on Pt/TiO_2 was 5.5 times higher than on Pt/CeO_2. This drastic increase of the density of adsorbed C_3H_8 molecules around the metallic Pt active sites would explain the high TOF values observed on Pt/TiO_2 because the reaction is positive order with respect to propane. The propylene oxidation turnover rate trend was $Pt/CeO_2 > Pt/Al_2O_3 \cong Pt/TiO_2$. Kinetic studies showed that on the three catalysts the apparent activation energy of propylene oxidation was about the same while the reaction orders were positive in oxygen and negative or zero in propylene. The higher activity of Pt/CeO_2 catalyst was explained by considering that the Pt-catalyzed reduction of ceria forms oxygen vacancies that would improve the mobility of lattice oxygen of the support and its transfer to the propylene species adsorbed on the metal.

1. Introduction

Catalytic oxidation on supported noble metals is an efficient technology for the abatement of small amounts of volatile organic compounds (VOCs) present in gaseous or liquid emissions [1,2]. In particular, Pt-based catalysts are highly active for oxidative removal of hydrocarbons [3–5]. However, stable lower alkanes such as methane or propane require relatively high temperatures to be completely oxidized over conventional Pt/Al_2O_3 catalysts and considerable effort has been devoted to find suitable supports or promoters for improving the intrinsic platinum oxidation activity. Fundamental knowledge on the oxidation mechanism is a prerequisite in order to design more active catalyst for hydrocarbon combustion. However, the oxidation reaction mechanism is largely dependent on the nature of the hydrocarbon molecule to be abated. For example, on Pt catalysts the oxidation of aromatics (benzene, toluene), naphtenics (cyclopentane), and olefins (ethylene, propylene,) is positive order in oxygen and negative or zero order in the hydrocarbon [6–10]; in contrast the C_2–C_4 alkane combustion is positive order with respect to alkane and negative or zero order in oxygen [11,12].

In this work we study the deep oxidation of propane and propylene on Pt supported on Al_2O_3, CeO_2 and TiO_2. Specifically, we compare the catalytic performance of Pt supported on nonreducible (Al_2O_3) and reducible (CeO_2, TiO_2) oxides for oxidizing two different hydrocarbons with the same number of C atoms. The aim was to ascertain the effect and role of support in the hydrocarbon oxidation mechanism that essentially takes place on metallic platinum. In particular, we investigate if the generation of reduced

* Corresponding authors. Tel.: +54 342 4555279: fax: +54 342 4531068.
E-mail addresses: capesteg@fiq.unl.edu.ar (C.R. Apesteguía), tgaretto@fiq.unl.edu.ar (T.F. Garetto).
[1] http://www.fiq.unl.edu.ar/gicic

1385-8947/$ - see front matter © 2013 Elsevier B.V. All rights reserved.
http://dx.doi.org/10.1016/j.cej.2013.12.006

species on the support (Ce^{3+} and Ti^{3+} species in ceria and titania, respectively) may interact with the Pt active sites and enhance its intrinsic activity for propane/propene deep oxidations. The increase of the Pt activity on reducible supports has been observed in redox reactions such as the water-gas shift reaction [13,14]. In the case of propane combustion, it has been reported that the activity of conventional Pt/Al_2O_3 catalysts may be improved by alumina sulfation [15,16] or by the addition of electrophilic additives [17]. Other authors have observed that the propane oxidation activity on Pt is enhanced when the metal is supported on more acidic supports [18,19]. Besides, we have found that the propane oxidation turnover rate is drastically increased when Pt is supported on acid zeolites as compared to Pt/Al_2O_3 [20]. The combustion of propylene has also been widely investigated on Pt-based catalysts because is a major pollutant in vehicle exhausts. Nevertheless, most of these studies have been performed on Pt/Al_2O_3 catalysts [9,21–25]. Very few papers deal with the combustion of propylene on Pt supported on reducible oxides such as CeO_2 [26] or TiO_2 [27].

2. Experimental

2.1. Catalyst preparation

Commercial samples of TiO_2 (Degussa P25, 50 m^2/g), γ-Al_2O_3 (Cyanamid-Ketjen CK300, 180 m^2/g) and CeO_2 (Rhodia HSA5, 240 m^2/g) were used as supports. Prior to impregnation with Pt salts, the supports were calcined in air at 873 K during 4 h. Platinum supported catalysts were prepared by incipient-wetness impregnation of supports at room temperature, using aqueous solution of tetramine platinum nitrate, $Pt(NH_3)_4(NO_3)_2$ (Aldrich, 99.99%). After impregnation, samples were dried overnight at 373 K and then calcined at 673 K in air for 4 h. Pt loading was about 0.5% for all the samples.

2.2. Catalyst characterization

BET surface areas (Sg) were measured by N_2 physisorption at 77 K using a Quantachrome Autosorb-1 sorptometer. Samples were degassed at 523 K before carrying out the analysis. The solid crystalline structures were determined by X-ray diffraction (XRD) in the range of 2θ = 10–80°, using a Shimadzu XD-D1 diffractometer and Ni filtered Cu Kα radiation (λ = 1.540 Å). Platinum loadings were measured by atomic absorption spectrometry.

Acid site densities were determined by using temperature-programmed desorption (TPD) of NH_3. Samples (200 mg) were treated in He (~60 cm^3/min STP) at 773 K for 1.5 h and exposed to a 1% NH_3/He stream at 373 K until surface saturation. Weakly adsorbed NH_3 was removed by flushing with He at 373 K for 0.5 h. Temperature was then increased at 10 K/min and the NH_3 concentration in the effluent was measured by mass spectrometry (MS) in a Baltzers Omnistar unit.

The temperature-programmed reduction (TPR) experiments were performed in a Micromeritics AutoChem 2920 unit, using 5% H_2/Ar gaseous mixture at 60 cm/min. Samples (300 mg) were heated at 10 K/min from 298 to 953 K. Since water is formed during sample reduction, the gas exiting from the reactor was passed through a cold trap before entering the thermal conductivity detector.

The platinum dispersion (D_{Pt}) on Pt/TiO_2 and Pt/Al_2O_3 samples was determined by H_2 chemisorption at 298 K using a conventional vacuum unit. Catalysts were reduced in H_2 at 573 K for 2 h and then outgassed for 2 h at 773 K prior to performing gas chemisorption experiments. Hydrogen uptake was determined using the double isotherm method as detailed in a previous work [28]. The hydrogen uptake on Pt/CeO_2 was measured by performing H_2 pulses at 223 K using a Micromeritics AutoChem II 2920 unit. In all the cases, an atomic H/Pt_s = 1 ratio, where Pt_s implies a Pt atom on surface, was used to calculate D_{Pt}.

Propane uptakes on Pt-based catalysts were measured at 298 K and 1.12 kPa in conventional vacuum equipment. Samples were reduced 1 h in H_2 at 673 K, then outgassed at this temperature for 1 h and finally cooled in vacuum to room temperature prior to performing the propane adsorption experiments.

2.3. Catalytic reactions

Hydrocarbon oxidation reactions were carried out in a tubular packed bed reactor (Pyrex, 0.8 cm ID) at atmospheric pressure. Samples were sieved to retain particles with 0.35–0.42 mm diameter and loaded to the reactor. Standard catalytic tests were performed at atmospheric pressure, using catalyst loadings (W) of 0.1 g, contact times (W/F^0_{HC}) of 12 g h/mol, and gas flow rates of 300 cc (STP)/min. Gaseous mixture compositions were: propane(propylene):O_2:N_2 = 0.8:9.9:89.3. On-line chromatographic analysis was performed using a gas chromatograph Shimadzu GC-8A equipped with a flame ionization detector and 23% SP-1700 Supelco packed column. Reactants and products were separated in the chromatographic column, then completely converted to methane by means of a methanation catalyst (Ni/Kieselghur) operating at 673 K, and finally detected by the flame ionization detector. Carbon monoxide was never detected in the effluent. Before catalytic measurements, all the catalysts were reduced in hydrogen at 673 K for 1 h and then cooled to the desired temperature. Pt-supported catalysts must be pretreated in H_2 to reduce the metal because PtO_2 species are not active for hydrocarbon combustion. Two experimental procedures were used for catalyst testing. The complete hydrocarbon oxidations were studied by obtaining curves of hydrocarbon conversion (X_{HC}) as a function of temperature (light-off curves). The temperature was raised at 3 K/min, from 373 K to 923 K. Kinetically-controlled X_{HC} versus time tests were performed at constant temperature: 523 K (propane) and 428 K (propylene). In all the cases, X_{HC} was lower than 10%. The products were sampled at 5 min intervals using an automated sampling valve.

3. Results and discussion

3.1. Support and catalyst characterization

The physicochemical properties of the samples are shown in Table 1. The support surface area did not change significantly by the addition of platinum. Fig. 1 shows the X-ray diffractograms of supports. Al_2O_3 exhibited the Bragg lines corresponding to diffraction of γ-Al_2O_3 phase while CeO_2 presented the peaks characteristics of cubic fluorite based structures. The main crystalline phase on TiO_2 was anatase, but the presence of an additional rutile phase was also detected. The support XRD patterns of Fig. 1 were not modified by the addition of Pt. Moreover, the X-ray diffractograms of Pt supported catalysts (not shown here) did not reveal the presence of crystalline Pt oxides, probably because of the low metal contents. The Pt dispersions on Pt/Al_2O_3 and Pt/TiO_2 determined by H_2 chemisorption at 298 K were 63% and 32%, respectively. The metal dispersion on Pt/CeO_2 (D_{Pt} = 50%) was determined by H_2 pulses at 223 K. The chemisorption of H_2 at low temperature (223 K) using H_2 pulses until saturation is widely employed for determining the Pt dispersion on ceria-supported Pt catalysts. This procedure turns negligible the H_2 spillover from the metal and gives the right Pt dispersion, as repeatedly proved in literature [29–31].

Table 1
Characterization of the catalysts used in this work.

Catalyst	% Pt	Sg (m^2/g)	D_{Pt} (%)	TPR (μmol H_2/g_{cat})[a]	TPD of NH_3 (n_a, μmol NH_3/m^2)	Propane uptake[b] (μmol/m^2)
Pt/Al_2O_3	0.51	175	63	0	0.132	0.057
Pt/CeO_2	0.49	220	50	938	0.461	0.038
Pt/TiO_2	0.48	50	32	29	1.310	0.208

[a] H_2 consumed by the support during the TPR of the catalysts.
[b] Propane uptakes measured at 298 K and P_P = 1.12 kPa.

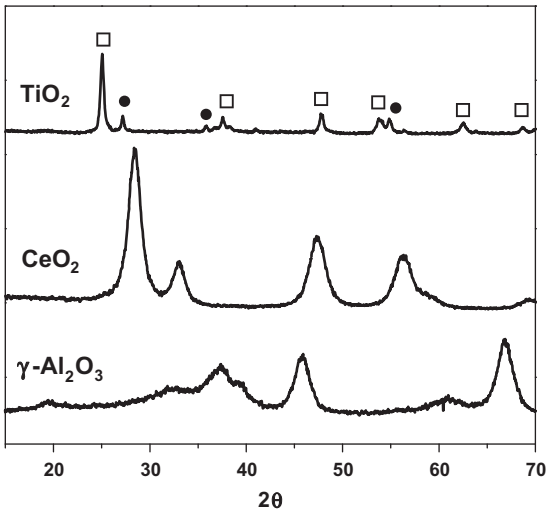

Fig. 1. X-Ray diffraction patterns of the supports. □ rutile; ● anatase.

The catalyst acid properties were probed by TPD of NH_3 preadsorbed at 373 K. The obtained TPD curves are shown in Fig. 2. The TPD traces for Pt/Al_2O_3 and Pt/CeO_2 exhibited the peak maxima between 443 and 543 K while the maximum temperature for the NH_3 TPD curve corresponding to Pt/TiO_2 appeared at about 653 K. The total amount of desorbed NH_3 was measured by deconvolution and integration of the TPD traces of Fig. 2 and it was taken as a measure of the total acid site density (n_a, μmol NH_3/m^2). The resulting n_a values are reported in Table 1. The sample acid site density increased from 0.132 μmol NH_3/m^2 on Pt/Al_2O_3 to 1.310 μmol NH_3/m^2 on Pt/TiO_2, i.e. by about one order of magnitude. In summary, results of Fig. 2 show that Pt/TiO_2 contains more and stronger surface acid sites as compared to Pt/Al_2O_3 or Pt/CeO_2.

The TPR profiles of catalysts with reducible supports (Pt/TiO_2 and Pt/CeO_2) are shown in Fig. 3. The TPR curve obtained for Pt/Al_2O_3 confirmed that alumina is a non-reducible support and is not included in Fig. 3. It is well established that the TPR profile of CeO_2 presents two reduction bands [32–34]: (i) a low-temperature band with a maximum at about 773 K that arises from the reduction of surface ceria, and (ii) a high-temperature reduction band with a maximum at around 1123 K that corresponds to the bulk reduction from CeO_2 to Ce_2O_3. Fig. 3 shows the TPR profile of Pt/CeO_2 up to 873 K. The reduction peak maximum corresponding to reduction of surface ceria appeared at 573 K, i.e. at a lower temperature as compared to that of CeO_2 support. This reduction peak shift is explained by taken into account that Pt catalyzes the surface reduction process of the support by activating at lower temperatures the dissociative adsorption of H_2 and thus generating reactive atomic protons. The TPR curve of Pt/TiO_2 in Fig. 3 exhibited a low temperature band centred at 373–393 K and a high-temperature band at about 573 K. The low-temperature band corresponds to the reduction of PtO_x species and the band at high temperature is due to the Pt-catalyzed reduction of surface Ti^{4+} species to Ti^{3+} via H_2 spillover [35,36]. Regarding the reducibility of TiO_2 support, no H_2 consumption peaks were detected when the sample was heated in 5% H_2 up to 773 K.

The support hydrogen consumptions determined from TPR profiles of Fig. 3 are presented in Table 1. The H_2 consumption for CeO_2 on Pt/CeO_2 was 938 μmol H_2/g_{cat}. This value was determined by subtracting the theoretical amount of H_2 consumed for reducing 0.49%Pt as PtO_2 from the total H_2 consumption obtained for Pt/CeO_2 in Fig. 3. By considering that H_2 was totally consumed for reducing Ce^{4+} to Ce^{3+} species, we inferred that on Pt/CeO_2 about 31% of the ceria support was reduced to Ce_2O_3. In contrast, the H_2 amount consumed in the high-temperature peak on Pt/TiO_2 was only 29 μmol H_2/g_{cat} indicating that less than 1% of Ti^{4+} species were reduced to Ti^{3+}.

The catalyst propane uptake capacity was determined at room temperature for a propane partial pressure of 1.12 kPa that was

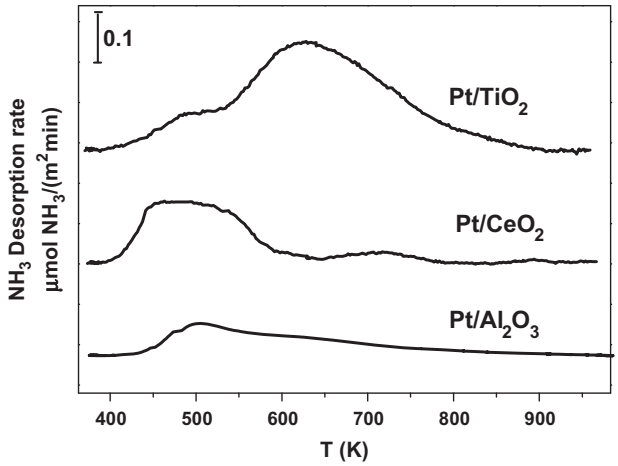

Fig. 2. TPD profiles of NH_3 on Pt catalysts. Heating rate: 10 K/min.

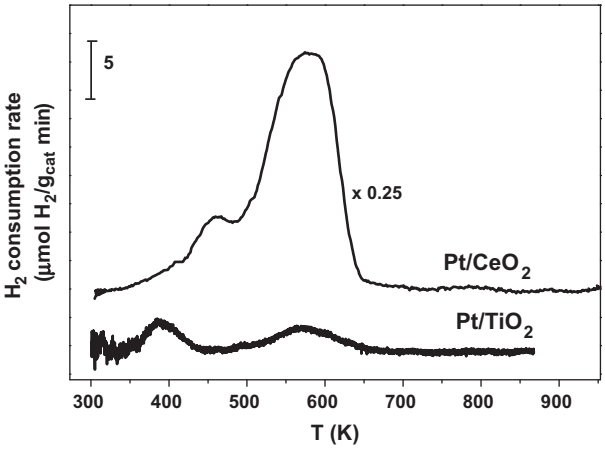

Fig. 3. TPR profiles of Pt-based catalysts. Heating rate: 10 K/min.

the hydrocarbon pressure used in catalytic tests. Results are shown in Table 1. The propane adsorption on Pt/TiO_2 (0.208 μmol/m^2) was about 3.6 times higher than on Pt/Al_2O_3 (0.057 μmol/m^2). The lowest propane uptake was determined on Pt/CeO_2 (0.038 μmol/m^2). The higher adsorption of propane on Pt/TiO_2 is probably associated with the higher acidity of this sample. Studies by FTIR of propane adsorption on TiO_2 and other oxides such as ZrO_2 have reported, in fact, that propane is essentially adsorbed on surface Lewis sites of these samples [37].

3.2. Catalytic activity

3.2.1. Propane oxidation

The light-off curves obtained for combustion of propane on the three catalysts used in this work are shown in Fig. 4. To quantitatively compare the catalyst oxidation activities, we measured from light-off curves the value of the temperature at $X_P = 50\%$, T^{50}; results are given in Table 2. Repeat profiles carried out with fresh samples confirmed the stability of the light-off temperatures. Table 2 shows that the T^{50} values for Pt/TiO_2 and Pt/CeO_2 were similar while that corresponding to Pt/Al_2O_3 was significantly higher. These T^{50} values were obtained from Fig. 4 per g of catalyst. When they are affected by the Pt dispersion, then the activity order is: $Pt/TiO_2 > Pt/CeO_2 > Pt/Al_2O_3$.

Catalysts were also tested for propane oxidation at constant temperature (523 K). In all the cases, the initial conversion of propane (X_P) was lower than 10% and the reaction was kinetically controlled. Results are shown in Fig. 5. Propane conversion remained approximately constant on Pt/Al_2O_3 and Pt/TiO_2 while continuously diminished on Pt/CeO_2 with the progress of the reaction. From the X_P versus time plots of Fig. 5 we determined the propane combustion rates per gram of Pt (r_P, mol propane/h g_{Pt}) and per surface Pt atom (TOF_p, h^{-1}). The observed deactivation for Pt/CeO_2 required that the initial conversion be determined by extrapolating the corresponding X_P vs time curve to initial time-on-stream. We compared the intrinsic Pt activity at initial conditions because we want to ascertain if the Pt activity is increased by the generation of reduced Ce^{3+} and Ti^{3+} species on the respective supports. The obtained r_P and TOF values are shown in Table 2. The r_p values followed the trend: $Pt/TiO_2 > Pt/CeO_2 > Pt/Al_2O_3$ Consistently, the TOF_p values were 1620 h^{-1}, 483 h^{-1} and 100 h^{-1}, on Pt/TiO_2, Pt/CeO_2 and Pt/Al_2O_3 respectively. These results in Table 2 showed that the Pt activity for propane oxidation is strongly affected by the nature of the support. It is worth noting that the propane oxidation turnover rate was about one order of magnitude higher when Pt was supported on titania than on alumina.

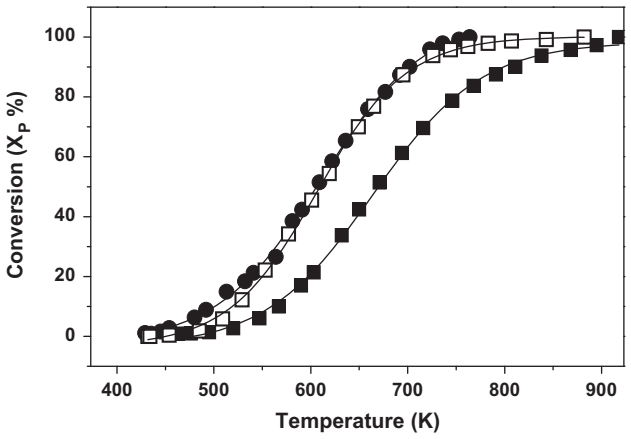

Fig. 4. Light-off curves for propane combustion. Pt/Al_2O_3 (■); Pt/TiO_2 (□); Pt/CeO_2 (●) [P = 101.3 kPa, W/F_p^0 = 4 g_{cat} h/mol, propane:O_2:N_2 = 0.8:9.9:89.3].

More fundamental kinetic data were obtained by calculating the reaction orders and apparent activation energies (E_a) for propane oxidation. The reaction orders were obtained by using a power-law rate equation:

$$r_p = kP_p^{\alpha}P_{o_2}^{\beta} \quad (1)$$

where P_p and P_{o_2} are the partial pressure of propane and oxygen in the feed, respectively. The α values were measured by varying the propane partial pressure between 0.5 and 2.0 kPa at a fixed oxygen pressure (14.2 kPa). Similarly, reaction order β was obtained by varying P_{o_2} between 5.1 and 20.3 kPa while keeping P_p at 1.1 kPa. The plots representing $\ln r_P$ as a function of $\ln P_p$ and $\ln P_{o_2}$ at 250 °C are shown in Fig. 6. The α and β values obtained from the plots of Fig. 6 are presented in Table 2. The reaction order with respect to propane was close to one on Pt/Al_2O_3 and Pt/CeO_2, and 1.5 on Pt/TiO_2, while the reaction order in oxygen was about zero on Pt/Al_2O_3 and Pt/CeO_2 but negative (−0.8) on Pt/TiO_2. These results are consistent with previous works reporting that lower-alkanes oxidation is positive order in the hydrocarbon and order zero or negative with respect to oxygen on Pt-based catalysts [11,38,39]. Propane adsorption on Pt is energetically competitive with oxygen [40] and a competitive propane/oxygen adsorption explains in a Langmuir–Hinshelwood mechanism the reaction inhibition by O_2, depending on the operating conditions used. In Fig. 7 we plotted the ln TOF_p values as a function of $1/T$ for determining the apparent activation energy and pre-exponential factor A for propane combustion on all the catalysts via an Arrhenius-type function. We obtained E_a from the slope of the resulting linear plots, and from the ordinate values at $1/T = 0$ we determined pre-exponential factors A. Results are shown in Table 2.

The reaction orders with respect to propane and oxygen were similar on Pt/CeO_2 and Pt/Al_2O_3 suggesting that the propane combustion reaction occurs via the same mechanism on both catalysts. According to literature [8,11,41], the rate-determining step for the low alkanes oxidation mechanism on platinum is the dissociative chemisorption of the alkane on Pt with the breakage of the weakest C–H bond followed by its interaction with oxygen atoms adsorbed on adjacent sites. Nevertheless, the apparent activation energy for propane oxidation was lower on Pt/CeO_2 than on Pt/Al_2O_3 (Table 2) and this would explain the higher activity observed on Pt/CeO_2. Probably, propane combustion on Pt/CeO_2 occurs not only on surface metallic Pt sites but also on perimeter Pt^0–Ce^{3+} sites of the metal-support interface providing an additional oxidation pathway. Formation of dual Pt^0–Ce^{3+} sites is favored by the high reducibility showed by CeO_2 in presence of Pt that generates a high concentration of surface Ce^{3+} sites. As we remarked above, our data show that about 30% of CeO_2 is reduced to Ce_2O_3 following the catalyst reduction treatment at 673 K before performing the catalytic tests. The assumption that Ce^{3+} sites are participating in the propane combustion mechanism is strongly supported by the fact that the Pt/CeO_2 activity continuously decreased on stream (see Fig. 5). This catalyst activity decay is easily interpreted by considering that the active Ce^{3+} sites are progressively consumed by reoxidation to Ce^{4+} in presence of an oxidative atmosphere containing oxygen and water.

The most active catalyst for propane combustion was Pt/TiO_2 that exhibited the highest values of both the activation energy, E_a, and the pre-exponential factor, A (Table 2). On the other hand, our results showed that Pt/TiO_2 is more acidic than Pt/CeO_2 and Pt/Al_2O_3 and that upon reduction in H_2 less than 1% of Ti^{4+} is reduced to Ti^{3+} (Table 1).

Differences in the support acid strength may influence the intrinsic oxidation Pt activity. Yazawa et al. [18,19] studied the propane combustion on Pt supported on different supports and observed that the propane oxidation activity on platinum increased

Table 2
Propane oxidation: catalytic results.

Catalyst	Light-off curves T^{50} (K)	Kinetically controlled catalytic tests					
		r_P (mol/h g_{Pt})	TOF_P (h^{-1})	Reaction orders		E_a (kJ/mol)	A (1/h.atm$^{(\alpha+\beta)}$)
				α	β		
Pt/Al_2O_3	668	0.32	100	0.8	0	60	5.94×10^7
Pt/CeO_2	606	1.21	483	0.9	0.1	37	1.83×10^6
Pt/TiO_2	603	2.66	1620	1.5	−0.8	84	2.15×10^{11}

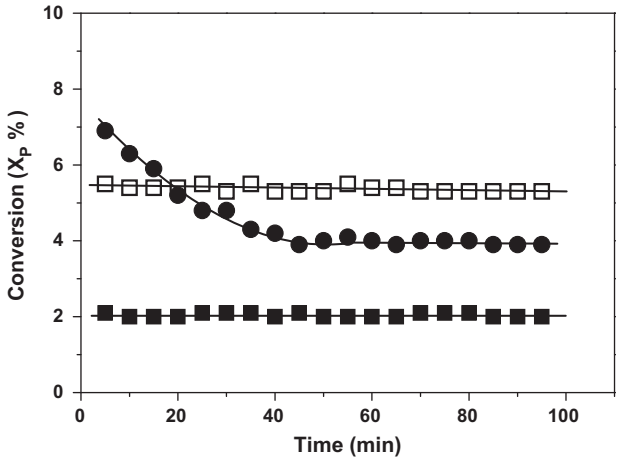

Fig. 5. Propane conversion as a function of time. Pt/Al_2O_3 (■), $W/F_P^0 = 12.3\ g_{cat}$ h/mol; Pt/TiO_2 (□), $W/F_P^0 = 4\ g_{cat}$ h/mol; Pt/CeO_2 (●), $W/F_P^0 = 12\ g_{cat}$ h/mol [$P = 101.3$ kPa, $T = 523$ K, propane:O_2:N_2 = 0.8:9.9:89.3].

with the acid strength. By reasoning that the Pt oxidation activity is higher when the metal is less oxidized, these authors proposed that platinum has higher oxidation-resistance in oxidizing atmospheres on more acidic support materials. In contrast, other authors that investigated the propane oxidation reaction over Pt supported on non-zeolitic materials did not find any correlation between the catalyst activity and the total acidity of the support [42,43]. Here, the most acidic catalyst (Pt/TiO_2) exhibited the highest propane combustion turnover rate and this result is consistent with the proposal of Yazawa et al. [18]. However, our data in Table 2 also show that the order with respect to oxygen on Pt/TiO_2 was negative (−0.8) and about zero for Pt/Al_2O_3 and Pt/CeO_2. This result is not consistent with the interpretation that Pt on electrophilic supports has the higher oxidation-resistance. In fact, if the effect of the acid supports is to prevent Pt from oxidation it is expected that the inhibition by oxygen would decrease with the support acid strength.

Results in Table 2 revealed that the areal propane uptake on Pt/TiO_2 is about 3.6 and 5.5 times higher than on Pt/Al_2O_3 and Pt/CeO_2, respectively. A drastic increase of the density of adsorbed propane species may promote the alkane oxidation rate and probably explains the high TOF values observed on Pt/TiO_2. In fact, a direct consequence of increasing the local propane concentration around the metallic Pt active sites would be the increase of the alkane oxidation conversion rate because the reaction is positive order with respect to the hydrocarbon. The adsorbed propane concentration increase on Pt/TiO_2 would also explain the drastic increase of the preexponential factor A that kinetically compensates the E_a augmentation observed for propane combustion on Pt/TiO_2 (Table 2). We have proposed a similar qualitative explanation (promotion of the alkane oxidation activity because of a drastic increase of the density of adsorbed alkane species) for the high activity observed on Pt/zeolite catalysts for the alkane oxidation reaction (excepting methane) [20].

3.2.2. Propylene oxidation

Fig. 8 shows the light-off curves obtained for combustion of propylene on our Pt-based catalysts. The T^{50} values obtained from these curves are presented in Table 3. The T^{50} values for Pt/Al_2O_3 and Pt/CeO_2 were similar while that corresponding to Pt/TiO_2 was significantly higher.

Propylene oxidation was also carried out on our Pt catalysts at constant temperature (428 K). Fig. 9 shows the evolution of propylene conversion as a function of time on the three catalysts investigated in this work. The propylene conversion remained constant on Pt/Al_2O_3 and Pt/TiO_2 but continuously decayed on Pt/CeO_2 with the progress of the reaction. The propylene oxidation rates, r_{pr}^0 and turnover frequencies, TOF_{Pr}, were determined from the X_{Pr} vs time curves of Fig. 9 and are presented in Table 3. Because of catalyst deactivation, the r_{pr}^0 and TOF_{Pr} values for Pt/CeO_2 were determined from the initial propylene conversion obtained by extrapolating the X_{Pr} vs time curve to initial time-on-stream. Data in Table 3 shows that the propylene oxidation turnover rate on Pt/CeO_2 (351 h^{-1}) was three times higher than on Pt/Al_2O_3 (118 h^{-1}) and Pt/TiO_2 (96 h^{-1}).

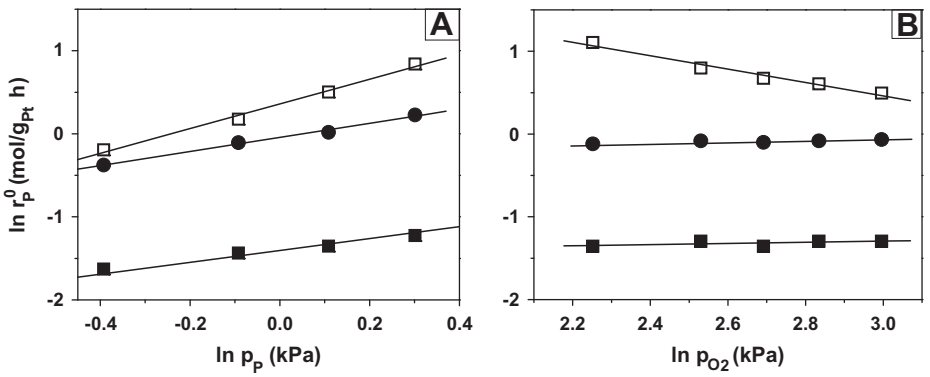

Fig. 6. Dependence of propane oxidation rate upon propane (A) and oxygen (B) partial pressure. Catalyst: Pt/TiO_2 (□), Pt/CeO_2 (●), Pt/Al_2O_3 (■) [$T = 523$ K, $P = 101.3$ kPa].

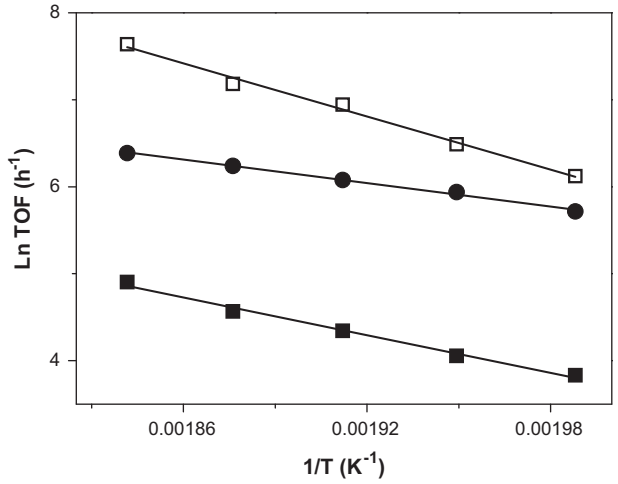

Fig. 7. Arrhenius plots for determining E_a (apparent activation energy) and A (pre-exponential factor). Propane oxidation turnover rates as a function of inverse temperature on Pt/TiO_2 (□), Pt/CeO_2 (●), Pt/Al_2O_3 (■) [P = 101.3 kPa, propylene:O_2:N_2 = 0.8:9.9:89.3].

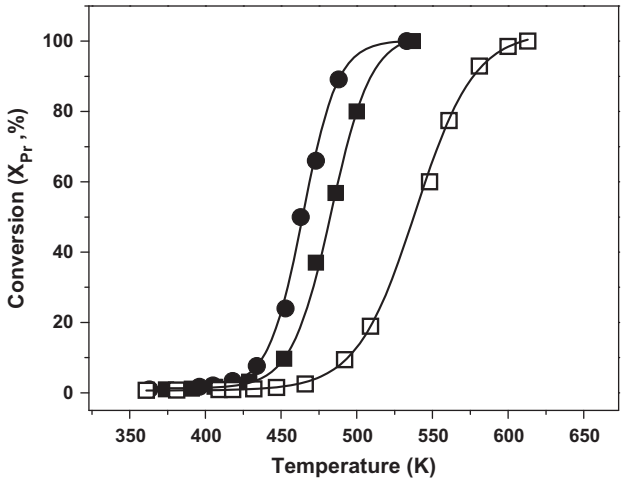

Fig. 8. Light-off curves for propylene combustion. Pt/Al_2O_3 (■); Pt/TiO_2 (□); Pt/CeO_2 (●) [P = 101.3 kPa, W/F_P^0 = 12 g h/mol, propylene:O_2:N_2 = 0.8:9.9:89.3].

In order to get insight on the reaction mechanism, we determined the reaction orders and activation energies for propylene oxidation. The influence of reactant partial pressure on catalyst activity was studied at 428 K. The propylene partial pressure was varied between 0.7 and 1.4 kPa maintaining the O_2 pressure at 14.7 kPa , while P_{o_2} was varied between 6.7 and 20 kPa at P_{Pr} = 1.1 kPa. The reaction orders, α and β, were determined using the linearized form of Eq. (2) that represents the propylene oxidation rate:

$$r_{pr} = kP_{pr}^{a}P_{o_2}^{b} \quad (2)$$

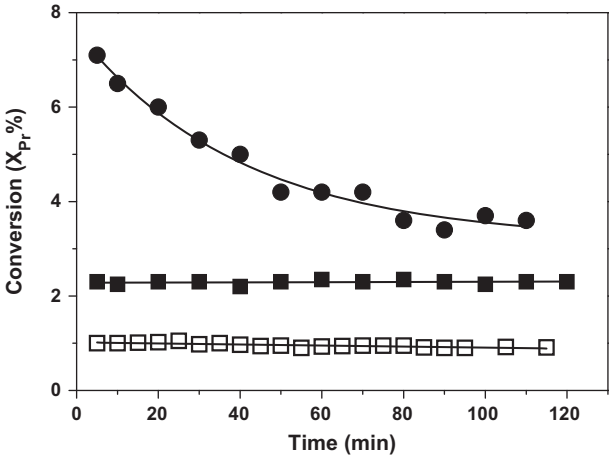

Fig. 9. Propylene conversion as a function of time. Pt/Al_2O_3 (■); Pt/TiO_2 (□); Pt/CeO_2 (●) [P = 101.3 kPa, T = 428 K, W/F_P^0 = 12 g h/mol, propylene:O_2:N_2 = 0.8:9.9:89.3].

The obtained values of α and β are shown in Table 3. In Table 3 we have also included the values of the apparent activation energy, E_a, and the pre-exponential factor, A, determined from ln TOF_{Pr} vs 1/T plots (not shown here).

The kinetic data in Table 3 shows that the order in propylene was negative on Pt/Al_2O_3 (−0.5) and close to zero on Pt/TiO_2 and Pt/CeO_2. The order in oxygen was positive on the three catalysts: 0.5 on Pt/CeO_2 and close to one on Pt/Al_2O_3 and Pt/TiO_2. Overall, we observe that the reactant order values in Table 3 are in agreement with data in literature for propylene oxidation on Pt-based catalysts [9,21,25–27]. On Pt/Al_2O_3, Shinjoh et al. [9] reported orders with respect to propylene and O_2 of −0.7 and 1.1, respectively, while Benard et al. [25] observed values of α = −0.5 and β = 1.1. On Pt/TiO_2, Baylet et al. [27] reported orders in propylene and oxygen of zero and 1.5, respectively. On Pt/CeO_2–Al_2O_3. Yu Yao [26] determined values of α = −0.3 and β = 1.2. The negative or zero orders with respect to propylene determined on our Pt-based catalysts reveal that propylene or derived-intermediates are strongly adsorbed on platinum causing self-inhibition. Pioneer studies on ethylene and propylene oxidation mechanism performed on Pt single crystals and foils [44–47] have proposed that the olefin is adsorbed and dehydrogenated to a surface intermediate that is consecutively oxidized to water and CO_2 by coadsorbed atomic oxygen. In the case of propylene, the intermediate would be 1-methylvinyl species adsorbed nearly parallel to the surface [46]. In this mechanism, the activation of the oxygen molecule would be the rate-limiting step which is in agreement with the positive order in oxygen determined on our Pt-supported catalysts. Consistently, Cant and Hall [48] observed that the order of activity of noble metals for oxidizing propylene depends upon the ability of the metal to activate O_2.

Results in Table 3 also show that the apparent activation energies were similar on the three catalysts used in this work, between

Table 3
Propylene oxidation: catalytic results.

Catalyst	Light-off curves T^{50} (K)	Kinetically controlled catalytic tests					
		r_{Pr} (mol/h g_{Pt})	TOF_{Pr} (h^{-1})	Reaction orders		E_a (kJ/mol)	A (1/h.atm$^{(\alpha+\beta)}$)
				α	β		
Pt/Al_2O_3	479	0.38	118	−0.5	1.1	43	2.24×10^6
Pt/CeO_2	463	0.88	351	0.1	0.5	39	2.62×10^6
Pt/TiO_2	538	0.16	96	−0.1	0.9	37	1.58×10^5

37 and 43 kJ/mol, thereby suggesting that propylene is oxidized via the same reaction mechanism. Nevertheless, the initial propylene oxidation turnover rate was higher on Pt/CeO_2 than on Pt/Al_2O_3 or Pt/TiO_2. This result may be explained by considering that the Pt-catalyzed reduction of ceria forms oxygen vacancies, in close vicinity to the Pt particles, which would improve both the lability and mobility of lattice oxygen of the support. The transfer of additional activated oxygen from the support to the adsorbed propylene species on the metal will increase the catalyst activity because the reaction is positive order in oxygen. A similar explanation relating the oxygen deficiency in ceria with a high catalytic activity has already been advanced for the deep oxidation of methane by other authors [49]. Finally, it must be noted that, as in the case of propane oxidation, the activity for propylene oxidation diminished with the progress of the reaction reflecting the loss of surface active sites on stream. Again, this activity decay probably reflects the filling of the oxygen vacancies on the support by reoxidation of Ce^{3+} sites under the oxidative atmosphere occurring during propylene oxidation.

4. Conclusions

The activity and reaction mechanism of the deep oxidation of propane and propylene on Pt/Al_2O_3, Pt/CeO_2 and Pt/TiO_2 catalysts depend on the nature of both the reactant and the support. For propane oxidation, the reaction orders are zero or negative in oxygen and positive in the hydrocarbon, which is in agreement with the assumption that the rate-limiting step of the reaction mechanism is the dissociative chemisorption of propane on platinum with the breakage of the weakest C–H bond. The catalyst activity trend for propane combustion is $Pt/TiO_2 > Pt/CeO_2 > Pt/Al_2O_3$. The propane uptake on Pt/TiO_2 is clearly higher than on Pt/CeO_2 or Pt/Al_2O_3. This drastic increase in the concentration of adsorbed propane species may explain the superior combustion activity obtained on Pt/TiO_2 because the reaction is positive order with respect to propane. On the other hand, the higher activity obtained on Pt/CeO_2 than on Pt/Al_2O_3 probably reflects the fact that the combustion of C_3H_8 on Pt/CeO_2 would occur not only on surface metallic Pt sites but also on perimeter Pt^0–Ce^{3+} sites providing an additional oxidation pathway.

For propylene oxidation, the reaction orders are positive in oxygen and zero or negative with respect to propylene. Propylene is strongly adsorbed on platinum causing self-inhibition and then is converted to water and CO_2 by coadsorbed activated oxygen. Propylene oxidation turnover rates follow the order: $Pt/CeO_2 > Pt/Al_2O_3 \cong Pt/TiO_2$. The superior activity of Pt/CeO_2 is interpreted by taken into account that the Pt-catalyzed reduction of ceria forms oxygen vacancies, in close vicinity to the Pt particles, which would improve both the lability and mobility of lattice oxygen of the support. The transfer of additional activated oxygen from the support to the adsorbed propylene species on the metal will increase the catalyst activity because the reaction is positive order in oxygen.

The oxidation activity for both hydrocarbons is stable on Pt/Al_2O_3 and Pt/TiO_2 but continuously decreases on Pt/CeO_2 with the progress of the reaction. This activity decay on Pt/CeO_2 is explained by considering that the surface active sites generated on the support by the Pt-catalyzed reduction of ceria (Ce^{3+} and oxygen vacancies sites) are consumed on stream because of the presence of an oxidative atmosphere containing oxygen and water.

Acknowledgements

This work was supported by the Universidad Nacional del Litoral (UNL), Consejo Nacional de Investigaciones Científicas y Técnicas (CONICET), and Agencia Nacional de Promoción Científica y Tecnológica (ANPCyT), Argentina.

References

[1] J.J. Spivey, Complete catalytic oxidation of volatile organics, Ind. Eng. Chem. Res. 26 (1987) 2165–2180.
[2] R.M. Heck, R.J. Farrauto, Catalytic air pollution control: Commercial technology, 1st Ed., Van Nostrand Reinhold, New York, 1995.
[3] A.B. Kooh, W.J. Han, R.G. Lee, R.F. Hicks, Effect of catalyst structure and carbon deposition on heptane oxidation over supported platinum and palladium, J. Catal. 130 (1991) 374–391.
[4] T.F. Garetto, M.S. Avila, C.I. Vignatti, V. Venkat, K. Rao, C.R. Chary, Apesteguía, Deep oxidation of benzene on Pt/V2O5–TiO2 catalysts, Catal. Lett. 130 (2009) 476–480.
[5] L.F. Liotta, Catalytic oxidation of volatile organic compounds on supported noble metals, Appl. Catal. B: Environ. 100 (2010) 403–412.
[6] K.T. Chuang, S. Cheng, S. Tong, Removal and destruction of benzene, toluene, and xylene from wastewater by air stripping and catalytic oxidation, Ind. Eng. Chem. Res. 31 (1992) 2466–2472.
[7] T.F. Garetto, C.R. Apesteguía, Structure sensitivity and in situ activation of benzene combustion on Pt/Al_2O_3 catalysts, Appl. Catal. B: Environ. 32 (2001) 83–94.
[8] T.F. Garetto, C.R. Apesteguía, Oxidative catalytic removal of hydrocarbons over Pt/Al_2O_3 catalysts, Catal. Today 62 (2000) 189–199.
[9] H. Shinjoh, H. Muraki, Y. Fujitani, Periodic operation effects in propane and propylene oxidation over noble metal catalysts, Appl. Catal. 49 (1989) 195–204.
[10] C. Pliangos, I.V. Yentekakis, V.G. Papadakis, C.G. Vayenas, X.E. Verykios, Support-induced promotional effects on the activity of automotive exhaust catalysts: 1. The case of oxidation of light hydrocarbons (C_2H_4), Appl. Catal. B: Environ. 14 (1997) 161–173.
[11] M. Aryafar, F. Zaera, Kinetic study of the catalytic oxidation of alkanes over nickel, palladium, and platinum foils, Catal. Lett. 48 (1997) 173–183.
[12] T.F. Garetto, E. Rincón, C.R. Apesteguía, The origin of the enhanced activity of Pt/zeolites for combustion of C_2–C_4 alkanes, Appl. Catal. B: Environ. 73 (2007) 65–72.
[13] G. Avgouropoulos, T. Ioannides, D.I. Kondarides, P. Panagiotopouloua, J. Papavasiliou, Water–gas shift activity of doped Pt/CeO_2 catalysts, Chem. Eng. J. (134) (2007) 16–22.
[14] K.G. Azzam, I.V. Babich, K. Seshan, L. Lefferts, Bifunctional catalysts for single stage water-gas shift reaction in fuel cell applications. Part 1. Effect of the support on the reaction sequence, J. Catal. 251 (2007) 153–162.
[15] A.F. Lee, K. Wilson, R. Lambert, C.P. Hubbard, R.G. Hurley, R.W. McCabe, H.S. Gandhi, The origin of SO_2 promotion of propane oxidation over Pt/Al_2O_3 catalysts, J. Catal. 184 (1999) 491–498.
[16] A. Hinz, M. Skoglundh, E. Fridell, A. Andersson, An investigation of the reaction mechanism for the promotion of propane oxidation over Pt/Al_2O_3 by SO_2, J. Catal. 201 (2001) 247–257.
[17] Y. Yasawa, H. Yhosida, S. Komai, T. Hattori, The additive effect on propane combustion over platinum catalyst: control of the oxidation-resistance of platinum by the electronegativity of additives, Appl. Catal. A: Gen. 233 (2002) 113–124.
[18] Y. Yazawa, N. Takagi, H. Yoshida, S. Komai, A. Satsuma, T. Tanaka, S. Yoshida, T. Hattori, The support effect on propane combustion over platinum catalyst: control of the oxidation-resistance of platinum by the acid strength of support materials, Appl. Catal. A: Gen. 233 (2002) 103–112.
[19] Y. Yazawa, H. Yoshida, T. Hattori, The support effect on platinum catalyst under oxidizing atmosphere: improvement in the oxidation-resistance of platinum by the electrophilic property of support materials, Appl. Catal. A: Gen. 237 (2002) 139–148.
[20] T.F. Garetto, E. Rincón, C.R. Apesteguía, Deep oxidation of propane on Pt-supported catalysts: drastic turnover rate enhancement using zeolite supports, Appl. Catal. B: Environ. 48 (2004) 167–174.
[21] L.M. Carballo, E.E. Wolf, Crystallite size effects during the catalytic oxidation of propylene on Pt/γ-Al_2O_3, J. Catal. 87 (1978) 366–373.
[22] A. Aznarez, F.C.C. Assis, A. Gil, S.A. Korili, Effect of the metal loading on the catalytic combustion of propene over palladium and platinum supported on alumina-pillared clays, Catal. Today 176 (2011) 328–330.
[23] H.-C. Wu, L.-C. Liu, S.-M. Yang, Effects of additives on supported noble metal catalysts for oxidation of hydrocarbons and carbon monoxide, Appl. Catal. A: Gen. 211 (2001) 159–165.
[24] M. Haneda, T. Watanabe, N. Kamiuchi, M. Ozawa, Effect of platinum dispersion on the catalytic activity of Pt/Al_2O_3 for the oxidation of carbon monoxide and propene, Appl. Catal. B: Environ. 142–143 (2013) 8–14.
[25] S. Benard, A. Baylet, Ph. Vernoux, J.L. Valverde, A. Giroir-Fendler, Kinetics of the propene oxidation over a Pt/alumina catalyst, Catal. Commun. 36 (2013) 63–66.
[26] Y.F. Yu Yao, The oxidation of CO and hydrocarbons over noble metal catalysts, J. Catal. 87 (1984) 152–162.
[27] A. Baylet, C. Capdeillayre, L. Retailleau, J.L. Valverde, Ph. Vernoux, A. Giroir-Fendler, Parametric study of propene oxidation over Pt and Au catalysts supported on sulphated and unsulphated titania, Appl. Catal. B: Environ. 102 (2011) 180–189.

[28] A. Borgna, T.F. Garetto, C.R. Apesteguía, F. Le Normand, B. Moraweck, Sintering of chlorinated Pt/γ-Al_2O_3 catalysts: An in situ study by X-Ray absorption spectroscopy, J. Catal. 186 (1999) 433–441.
[29] V. Perrichon, L. Retailleau, P. Bazin, M. Daturi, J.C. Lavalley, Metal dispersion of CeO_2–ZrO_2 supported platinum catalysts measured by H_2 or CO chemisorption, Appl. Catal. A: Gen. 260 (2004) 1–8.
[30] S. Nousir, S. Keav, J. Barbier Jr., M. Bensitel, R. Brahmi, D. Duprez, Deactivation phenomena during catalytic wet air oxidation (CWAO) of phenol over platinum catalysts supported on ceria and ceria–zirconia mixed oxides, Appl. Catal. B: Environ. 84 (2008) 723–731.
[31] Ch. Vignatti, M.S. Avila, C.R. Apesteguía, T.F. Garetto, Catalytic and DRIFTS study of the WGS reaction on Pt-based catalysts, Int. J. Hydrog. Energy 35 (2010) 7302–7312.
[32] H.C. Yao, Y.F.Y. Yao, Ceria in automotive exhaust catalysts: I. Oxygen storage, J. Catal. 86 (1984) 254–265.
[33] G. Jacobs, U.M. Graham, E. Chenu, P.M. Patterson, A. Dozier, B.H. Davis, Low-temperature water-gas shift: impact of Pt promoter loading on the partial reduction of ceria and consequences for catalyst design, J. Catal. 229 (2005) 499–512.
[34] S. Letichevsky, C.A. Tellez, R.R. De Avillez, M.I.P. Silva, M.A. Fraga, L.G. Appel, Obtaining CeO_2–ZrO_2 mixed oxides by coprecipitation: role of preparation conditions, Appl. Catal. B: Environ. 58 (2005) 203–210.
[35] T. Huizinga, J. van Grondelle, R. Prins, A temperature programmed reduction study of Pt on Al_2O_3 and TiO_2, Appl. Catal. 10 (1984) 199–213.
[36] J.C. Conesa, J. Soria, Reversible titanium (3+) formation by hydrogen adsorption on M/anatase (TiO_2) catalysts, J. Phys. Chem. 86 (1982) 1392–1395.
[37] M.A. Hasan, M.I. Zaki, L. Pasupulety, IR Investigation of the oxidation of propane and likely C_3 and C_2 products over group IVB metal oxide catalysts, J. Phys. Chem. B 106 (2002) 12747–12756.
[38] Y. Yazawa, N. Kagi, S. Komai, A. Satsuma, Y. Murakami, T. Hattori, Kinetic study of support effect in the propane combustion over platinum catalyst, Catal. Lett. 72 (2001) 157–160.
[39] R. Burch, T.C. Watling, Kinetics and Mechanism of the Reduction of NO by C_3H_8 over Pt/Al_2O_3 under lean-burn conditions, J. Catal. 169 (1997) 45–54.
[40] Y.Y. Yao, Oxidation of alkanes over noble metal catalysts, Ind. Eng. Chem. Prod. Res. Dev. 19 (1980) 293–298.
[41] L. Hiam, H. Wise, S. Chaikin, Catalytic oxidation of hydrocarbons on platinum, J. Catal. 10 (1968) 272–276.
[42] C.P. Hubbard, K. Otto, H.S. Gandhi, K.Y. Ng, Effects of support material and sulfation on propane oxidation activity over platinum, J. Catal. 144 (1993) 484–494.
[43] R. Burch, E. Halpin, M. Hayes, K. Ruth, J.A. Sullivan, The nature of activity enhancement for propane oxidation over supported Pt catalysts exposed to sulphur dioxide, Appl. Catal. B: Environ. 19 (1998) 199–207.
[44] P. Berlowitz, C. Megiris, J.B. Butt, H.H. Kung, Temperature-programmed desorption study of ethylene on a clean, a hydrogen-covered, and an oxygen-covered platinum (1 1 1) surface, Langmuir 1 (1985) 206–212.
[45] U. Ackelid, L. Olsson, L.G. Petersson, Ethylene oxidation on polycrystalline platinum over eight orders of magnitude in ethylene pressure: A kinetic study in the viscous pressure regime, J. Catal. 161 (1996) 143–155.
[46] A.M. Gabelnick, J.L. Gland, Propylene deep oxidation on the Pt (111) surface: temperature programmed studies over extended coverage ranges, Surf. Sci. 440 (1999) 340–350.
[47] A.M. Gabelnick, A.T. Capitano, S.M. Kane, J.L. Gland, D.A. Fischer, Propylene oxidation mechanisms and intermediates using in situ soft X-ray fluorescence methods on the Pt (1 1 1) Surface, J. Am. Chem. Soc. 122 (2000) 143–184.
[48] N.W. Cant, W.K. Hall, Catalytic oxidation: II. Silica supported noble metals for the oxidation of ethylene and propylene, J. Catal. 16 (1970) 220–231.
[49] C. Bozo, N. Guilhaume, J.M. Herrmann, Role of the ceria–zirconia support in the reactivity of platinum and palladium catalysts for methane total oxidation under lean conditions, J. Catal. 203 (2001) 393–406.